Nuclear-magnetic-resonance powder patterns in Al_6Mn, Al_4Mn, and $Al_{12}Mn$ polycrystals

G. H. Stauss, M. Rubinstein, and E. J. Friebele
Naval Research Laboratory, Washington, D.C. 20375-5000

L. H. Bennett and R. J. Schaefer
National Bureau of Standards, Gaithersburg, Maryland 20899
(Received 15 September 1986)

The room-temperature nuclear-magnetic-resonance (NMR) spectra of polycrystalline $Al_{12}Mn$, Al_6Mn, and Al_4Mn have been obtained. A resonance line-shape simulation computer program was utilized to obtain the Hamiltonian parameters which characterize these powder patterns. These three compositions were chosen for study because various workers have suggested that a relationship exists between the quasiperiodic icosahedral Al-Mn structure and one or another of these three Al-Mn compounds. After acquiring the NMR spectra of these three compounds, and obtaining their quadrupole coupling and Knight-shift parameters, we conclude that, based on the NMR data, the microscopic structure of quasiperiodic Al-Mn bears little resemblance to any of the compounds studied.

INTRODUCTION

Recently, Shechtman and co-workers reported[1] a new class of ordered solids which diffract electrons and x rays with sharp Bragg peaks but possesses icosahedral symmetry inconsistent with translational crystalline invariance. This long-range order with fivefold rotational symmetry elements was first found with the composition $Al_{86}Mn_{14}$, and then in Al-rich Al-Mn alloys stabilized with Si. (Similar ordering has been reported in other alloy systems.) There also exists a so-called T phase in the Al-Mn system which is translationally invariant in one direction and not in the other two.[2] These new classes of solids have been discussed variously in terms of Penrose tiling[3] and in terms of mass-density and Landau theory,[4] and in terms of projection from higher-dimensional spaces.[3]

The icosahedral-quasiperiodic phase was originally observed in samples nominally of Al_6Mn composition. Stern, Ma, and Bouldin[5] reported that extended x-ray absorption fine-structure (EXAFS) measurements performed on the icosahedral phase reveal a relationship between it and the orthorhombic Al_6Mn structure, and that the Mn atoms are in two different sites in the population ratio of the golden mean, $\tau=(1+\sqrt{5})/2$. The more populous site was found to be similar to that in the Al_6Mn crystal, but with bond-angle distortions, while the other site had additional bond-stretching distortions. Stern *et al.* found that the volume per Mn site is independent of the type of site, and is the same as in the Al_6Mn crystal. On the other hand, there is evidence that both the icosahedral and the T phases occur in a range of compositions closer to that of Al_4Mn, and it has been suggested that the structures of these phases bear some relationship to the Al_4Mn crystal structure[6]. Pauling[7] has suggested a relationship between the $Al_{12}Mn$ G phase and the icosahedral phase.

The purpose of the present communication is to present the nuclear-magnetic-resonance (NMR) spectra of polycrystalline Al_6Mn, Al_4Mn, and $Al_{12}Mn$ so that they may be compared to the previously published spectra of the icosahedral and "T" phases of Al-Mn.[8,9] We first discuss the crystalline structures of Al_6Mn, Al_4Mn and $Al_{12}Mn$ as determined by x-ray diffraction. We then discuss the NMR spectra, which were obtained at room temperature and at several frequencies, and display computer-generated simulations of these spectra. Finally, we discuss the relationship between these spectra and those of the quasiperiodic materials.

CRYSTAL STRUCTURE

A. Al_6Mn

Nicol[10] determined the structure of Al_6Mn by x-ray diffraction. A centered orthorhombic crystal with 28 atoms per unit cell was found with dimensions $a=7.55$, $b=6.50$, and $c=8.8$ Å. The space group is D_{17}^{2h} ($Cmcm$), and contains four units of Al_6Mn per unit cell. The unit cell contains four equivalent Mn atoms in site 4(c) with local symmetry mm, eight equivalent Al atoms in site 8(e) with local symmetry 2, eight equivalent Al atoms in site 8(g) with local site symmetry m, and another set 8(f) of eight equivalent Al atoms also with site symmetry m.

B. Al_4Mn

The phase commonly designated as Al_4Mn is hexagonal with $a=28.35$ Å and $c=12.36$ Å as originally determined by Hofmann[11] and confirmed by Taylor.[12] This phase was found by Phillips[13] to have a range of compositions but with an upper limit to its Mn content (31.5 wt. % Mn) which is less than the concentration given by the formula Al_4Mn (33.7 wt. % Mn). The historical designation of this phase as Al_4Mn is thus misleading, and the phase designated as "μ" (hexagonal, $a=19.95$ Å, $c=24.52$ Å) by Taylor has a composition (34.5 wt. % Mn) equally close to this formula. In fact, it

appears probable that the phase which Gödecke and Köster[14] have designated as Al_4Mn at 34 wt. % Mn on their phase diagram was actually the μ phase of Taylor.

Taylor[12] measured a density of approximately 3.5 g/cm^3 for alloys in the composition range of Al_4Mn, which indicates approximately 550 atoms in one hexagonal unit cell. Unfortunately, no studies of the arrangement of these atoms within the unit cell have been reported.

While neither the structure nor the range of stability of the Al_4Mn phase is well known, the phase is readily formed by growth from the melt or by annealing rapidly quenched samples of approximately 31 wt. % Mn. It has been found[7] that at moderately rapid growth rates ($\sim$1 cm/sec), Al_4Mn can form with a high density of defects, producing a structure with an electron diffraction pattern which suggests a relationship to the T (decagonal) phase. In addition, the composition of the icosahedral phase has been shown[7,15,16] to be close to that given by the formula Al_4Mn.

C. $Al_{12}Mn$

The crystal structure of $Al_{12}Mn$ (the G phase) has been determined by Adams and Rich.[17] The unit cell is body-centered cubic. There are two $Al_{12}Mn$ units per cell. The space group is T_h^5 ($Im3$). Two Mn atoms are placed in special positions 2(a) with cubic local symmetry, and 24 Al atoms are in positions 24(g), with symmetries lower than cubic. Each Mn is surrounded by an icosahedron of 12 aluminum atoms.

To form G-phase sample, a liquid aluminum alloy with 6.3 at. % Mn was first rapidly solidified by melt spinning to give a mixture of icosahedral phase and supersaturated fcc aluminum. During subsequent heating at 400 °C, the melt-spun material transforms within a few minutes to a fine-grained mixture of orthorhombic Al_6Mn crystalline phase plus saturated fcc aluminum which is stable above 520° C, but metastable below 500 °C. The G phase forms in about 1000 hours at 400 °C by the slow reaction of Al_6Mn with Al. We have succeeded in creating material that is more than 80 volume percent $Al_{12}Mn$, with the balance fcc aluminum containing less than 1 at. % Mn in solid solution.

POWDER PATTERNS

The random orientations in a polycrystalline or powdered specimen gives rise to a distribution of local environments at the nuclei which results from orientation-dependent interactions. The resulting resonance line is termed a powder pattern. In the present paper we are concerned with powder patterns which are produced by the combined action of the isotropic magnetic shift (Knight shift), anisotropic magnetic shift, and the nuclear quadrupole interaction.

The NMR Hamiltonian for a nuclear spin I in a magnetic field H situated in a site of less than axial symmetry in a metallic lattice can be written as

$$\mathcal{H} = -\gamma\hbar\mathbf{I}\cdot\mathbf{H} + (h\nu_q/6)[3I_z^2 - I^2 + \eta(I_x^2 - I_y^2)] - \gamma\hbar\mathbf{I}\cdot\vec{\vec{K}}\cdot\mathbf{H} ,$$

where $\mathcal{H}$ is the Hamiltonian.

In this equation ν_q is the quadrupole coupling, η the quadrupole asymmetry parameter, and $\vec{\vec{K}}$ is the Knight-shift tensor. The expression simplifies significantly for the case of axial symmetry where $\eta=0$ and the Knight shift can be expressed in terms of only two components, the isotropic and axial components, $K_{\rm iso}$ and $K_{\rm ax}$. This Hamiltonian gives rise in the perturbation limit to $2I$ observable resonant transitions in the NMR spectrum of each type of nuclear site. The magnetic field necessary to tune each transition, at constant frequency, is a function of the angles between the magnetic field and the axes of the Knight-shift and quadrupole tensors. A powder pattern line shape is the experimental result of combining spectra of crystallites distributed uniformly over all possible orientations.

It is possible to describe the powder pattern line shape analytically in the axially symmetric case.[18] While limited, this approach provides insight into the effects of the perturbing interactions. To simulate the general case, it is necessary to use a computer. Techniques have been developed by Taylor and Bray[19] to simulate a powder pattern numerically by calculating the resonance field (or frequency) for a finite number of steps in $\cos\theta$ and ϕ space, typically 100×100, and then histogramming the result on a magnetic field scale.

The resonance line-shape simulation program of Taylor and Bray[19] was originally written for a card-reading mainframe computer. We have adapted the computational routines of the code to function on a personal computer.[20] This code has been optimized for vectorization and an additional option of using a 64-bit array processor board has been incorporated, enabling experimental line shapes to be simulated efficiently. Finally, this input routine has been adapted for keyboard file entry and the output is provided to both the graphics monitor and digital plotter. Computer optimization of Hamiltonian parameters through least-squares fitting is a difficult process, often leading to nonphysical results, so the role of the program is to illustrate and verify the effects of parameters chosen by the operator. A more appropriate procedure is to select parameters based on a physical model and then to use the program to verify and refine the chosen parameters as well as to determine the sensitivity of the agreement between computer and experimental spectra to variations in the parameters. In the present paper, however, we arrive at the quadrupole parameters by judicious guessing of the original parameters, and then altering them so the calculated spectrum closely resembles the experimental spectrum.

A. Al_6Mn

The unit cell of Al_6Mn has a single type of Mn site and three inequivalent Al sites. Both the ^{27}Al and ^{55}Mn resonances were examined at room temperature. The NMR powder spectra were taken with a pulsed spectrometer us-

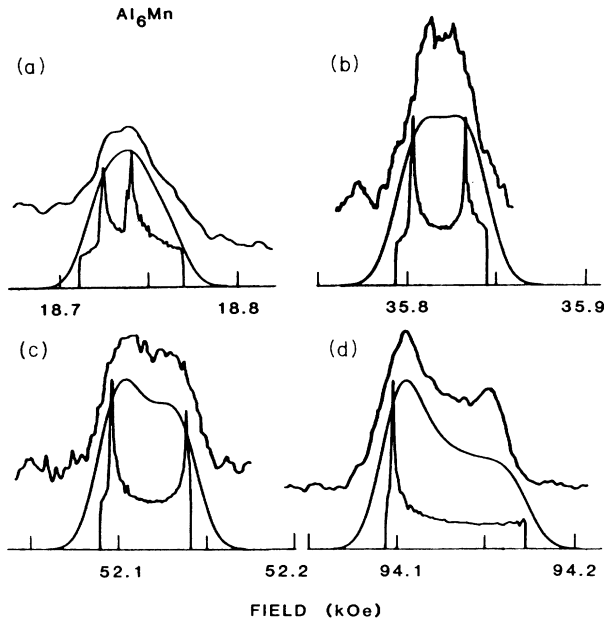

FIG. 1. NMR absorption spectra of ^{55}Mn in powdered Al_6Mn at room temperature. The four top traces are experimental; bottom, simulated with parameters of Table I; middle, simulated with 10-Oe additional Gaussian broadening. (a) 19.8 MHz, (b) 37.8 MHz, (c) 55.0 MHz, (d) 99.34 MHz.

ing coherent pulses and boxcar echo detection[20] to obtain absorption line shapes.

The ^{55}Mn powder spectra of Al_6Mn observed at room temperature and at constant frequencies of 19.8, 37.8, 55.0 and 99.34 MHz, are shown in Fig. 1. In each case, the uppermost spectrum is the experimental result, the lowest is the unbroadened theoretical powder pattern obtained by computer, and the middle spectrum is the same calculated pattern convoluted with a 10-G Gaussian-broadening function. The calculated spectra shown were all made with the parameters listed in Table I. The width of the spectrum is a minimum at the intermediate frequencies, and increases at the highest and the lowest frequencies. This can be explained by the presence of competing quadrupolar and anisotropic Knight-shift interactions. The quadrupolar interaction broadens the spectrum at low frequencies, whereas the anisotropic Knight shift broadens the spectrum at high frequencies.[18] A graph of the theoretical and experimental linewidth as a function of frequency is shown in Fig. 2. The theoretical curve uses the approximation of axial symmetry.[18]

TABLE I. Al_6Mn NMR fitting parameters.

Site	K_{iso}	K_{ax}	ν_q (MHz)	η
$Al_{(1)}$	0	0	1.4	1.0
$Al_{(2)}$	0	0	1.4	1.0
$Al_{(3)}$	0	0	1.4	0.2
Mn	$+50.7\times10^{-4}$	-2.7×10^{-4}	0.756	0.8

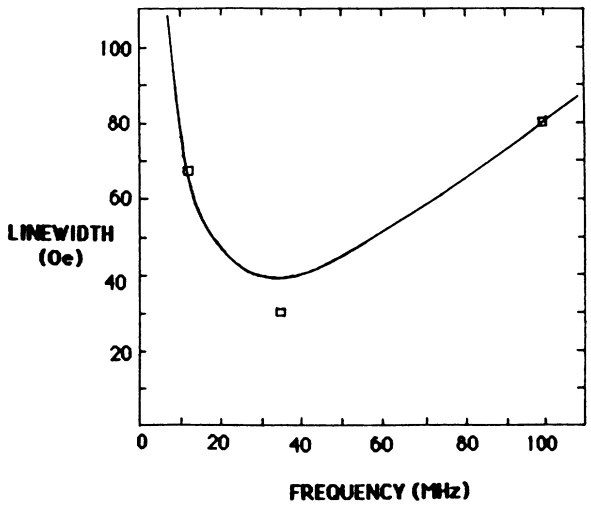

FIG. 2. Full width of ^{55}Mn central transition in Al_6Mn versus frequency (assuming $\eta=0$, $K_{ax}=2.74\times10^{-4}$, and $\nu_Q=0.746$ MHz). Squares are experimental data and line is the theoretical curve from Ref. 18.

A point-charge calculation of the electric field gradient at Mn sites, assuming the electric charges residing on all the Al and Mn sites to be $+1$ electronic charge, and using the nearest-neighbors only (defined by the Wigner-Seitz cell) is $\eta=0.08$ and $eq=0.68\times10^{+20}$ V/m^2. There exists a large discrepancy between the simple point-charge calculation and the experimentally obtained parameters. Agreement with point-charge calculation is not generally expected in a metal where long-range Ruderman-Kittel-Kasuya-Yosida (RKKY) effects are dominant.

The ^{27}Al spectrum of Al_6Mn is shown in Fig. 3. The width of the spectrum is observed to be inversely propor-

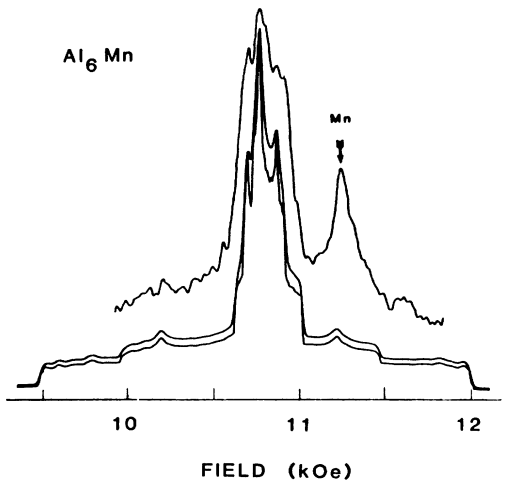

FIG. 3. NMR absorption spectrum of powdered Al_6Mn at 12 MHz, room temperature. Lowest trace simulates the ^{27}Al portion of the experimental trace (top) using parameters in Table I. This is broadened by 10 Oe in the middle trace.

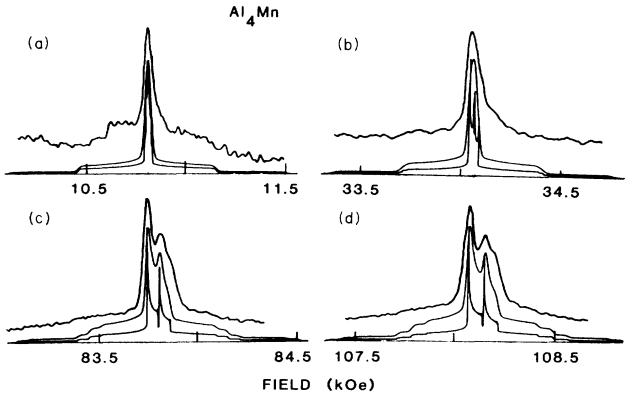

FIG. 4. Experimental and simulated NMR absorption spectra of ^{27}Al in Al_4Mn at room temperature. Bottom and middle simulations (10 Oe broadened), are drawn with parameters from Table II. (a) 12.0 MHz, (b) 37.8 MHz, (c) 93.0 MHz, (d) 120.0 MHz.

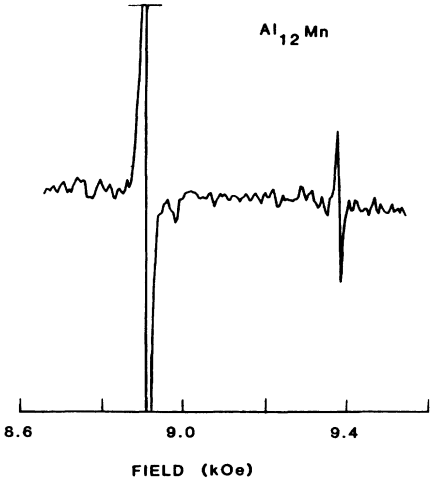

FIG. 5. NMR absorption derivative spectrum of powdered $Al_{12}Mn$ at room temperature, 9.90 MHz.

tional to the frequency, unlike that of the ^{55}Mn resonance, implying that the anisotropic Knight shift is negligible. For that reason, we show data for only a single frequency (12.0 MHz), since all the observed resonances have similar structure. The simulation to the overall ^{27}Al line shape from the three inequivalent Al sites was obtained with the parameters shown in Table I, where two of the sites are made equivalent. The value $K_{iso}=0$ represents a shift of -0.0017 with respect to the isotropic Knight shift of Al metal flakes, for which $K=+0.0017$.[21] The choice of the quadrupole coupling parameter is largely governed by the overall width of the pedestal on which the central peak stands.

B. Al_4Mn

In Al_4Mn, the ^{55}Mn resonance line could not be observed at any frequency. A possible explanation for its absence is that the Mn possesses a moment which broadens the ^{55}Mn resonance line. This is the explanation offered by Warren *et al.*[9] to explain the loss of intensity in the ^{55}Mn resonance of the icosahedral material. Alternative explanations for the absence of the ^{55}Mn signal in Al_4Mn are that Mn possesses a very large quadrupole splitting with a ν_q value of several MHz, or that it occupies several different sites with widely different Knight shifts.

The ^{27}Al resonance spectra of Al_4Mn taken at 12, 37, 98, and 120 MHz are illustrated in Fig. 4. These shapes differ markedly from those of Al_6Mn. The quadrupole coupling is significantly weaker, as indicated both by the width of the resonance pedestals and the lack of broadening at low fields. On the other hand, a progressive broadening and splitting is observed with increasing field. A simulation of these trends is shown in Fig. 4 based on the parameters of Table II. The agreement of the simulation with the data is quite good. Note that only two sites are assumed in the model and the two sites differ only in K_{iso}. The large asymmetries needed for fitting would suggest that the atoms are associated with a degree of selective clustering and directional bonding, i.e., in molecular groupings. The two-site fitting for Al_4Mn is undoubtedly a simplification; the resolution of the experimental spectrum is insufficient to determine a more-detailed distribution of parameters. When the structure of Al_4Mn is determined, it will be of interest to identify these two "sites" with the actual distribution of the sites in the unit cell.

C. $Al_{12}Mn$

The NMR spectra of $Al_{12}Mn$ were obtained using a field-modulated cw spectrometer. A pulsed spectrometer and coherent boxcar detection was also utilized. The pulsed spectrometer yields the absorption line shapes directly, while the cw spectrometer yields the absorption derivative. The ^{27}Al and ^{55}Mn absorption derivative spectrum at 9.9 MHz is shown in Fig. 5. The extremely narrow Mn width of the G phase indicates zero quadrupole interaction of the lattice with the Mn nuclei, as expected at a cubic site. The ^{27}Al resonance is largely masked by

TABLE II. ^{27}Al NMR parameters in Al_4Mn. K_1, K_2, and K_3 are the principal components of the Knight shift tensor.

Site	Weight	K_1 (10^{-4})	K_2 (10^{-4})	K_3 (10^{-4})	ν_Q (MHz)	η
1	3	−1.85	−1.85	+3.70	0.39	1.0
2	2	+6.45	+6.45	12.00	0.39	1.0

TABLE III. ^{27}Al and ^{55}Mn parameters in $Al_{12}Mn$.

Site	K_{iso}(%)	ν_Q (MHz)
Al	0.16	
Mn	0.5	0.0

the free Al component. Spectra taken with the pulsed spectrometer show indications of additional structure, but this is also considerably narrower than the corresponding Al spectrum from the icosahedral phase. Table III shows the NMR parameters deduced for $Al_{12}Mn$.

COMPARISONS WITH RESULTS IN THE QUASIPERIODIC CRYSTALS

In comparison with the ^{27}Al spectra at polycrystalline Al_6Mn and Al_4Mn, the powder patterns of the icosahedral and decagonal phases are much broader and lack definitive features. These quasiperiodic spectra have been reported previously by Warren *et al.*[9] and Rubinstein *et al.*[8] Warren *et al.* state that the icosahedral powder pattern implies the presence of a rather broad distribution of quadrupole coupling and asymmetry parameters. Both Rubinstein *et al.* and Warren *et al.* note that the ^{55}Mn resonance in the icosahedral phase does not exhibit the quadrupole structure to be expected if there were only two types of sites in the icosahedral phase, as might be inferred from the simplest interpretations of the mathematical models based on three-dimensional Penrose tilings. The basic conclusion concerning both Al and Mn resonance in the quasiperiodic structures is that there are broad distributions of local environments, with the T phase having the broadest of all.

The $Al_{12}Mn$ resonance is dissimilar from the resonance spectrum of the icosahedral phase. The contrast between the icosahedral results with Al_6Mn clearly shows the limited extent to which the microscopic structure of Al_6Mn can be said to resemble the quasiperiodic structure. On the other hand, certain parameters, the quadrupole coupling constants ν_q, and the isotropic Knight shift K_{iso}, do appear to be quite similar in these cases. When one looks at the Al_4Mn results the correspondences become fewer, being limited only to K_{iso} for the Al sites. Quadrupole coupling is significantly weaker at Al sites in Al_4Mn, while it may be very large at Mn sites. A number of investigators have raised the possibility that the chemical bonding in the quasiperiodic crystals is qualitatively different from the normal crystals. Our NMR results do not confirm this difference. The electronic and magnetic properties of icosahedral samples are those to be expected from the Al-Mn alloys, and are not peculiar to the icosahedral structure.

[1]D. Shechtman, I. A. Blech, D. Gratius, and J. W. Cahn, Phys. Rev. Lett. **53**, 1951 (1984).
[2]L. Bendersky, Phys. Rev. Lett. **55**, 1461 (1985).
[3]D. Levine and P. J. Steinhardt, Phys. Rev. Lett. **53**, 2477 (1984); V. Elser, Phys. Rev. B **32**, 4892 (1985).
[4]P. Bak, Phys. Rev. Lett. **54**, 1517 (1985); R. E. Watson and M. Weinert, Mater. Sci. Eng. **79**, 105 (1986).
[5]E. A. Stern, Y. Ma, and C. E. Bouldin, Phys. Rev. Lett. **55**, 2172 (1985). (Some of the conclusions of this reference have been subsequently modified.)
[6]L. Bendersky, R. J. Schaefer, F. S. Biancaniello, W. J. Boettinger, J. Kaufman, and D. Shechtman, Scr. Met. **19**, 909 (1985).
[7]L. Pauling, Nature **512**, (1985).
[8]M. Rubinstein, G. H. Stauss, T. E. Phillips, K. Moorjani, and L. H. Bennett, J. Mater. Res. **1**, 243 (1986).
[9]W. W. Warren, Jr., H. S. Chen, and J. J. Hauser, Phys. Rev. B **32**, 7614 (1985).
[10]A. D. I. Nicol, Acta Crystallogr. **6**, 285 (1953).
[11]W. Hofmann, Aluminum **20**, 865 (1938).
[12]M. A. Taylor, Acta. Metall. **8**, 256 (1960).
[13]H. W. L. Phillips, J. Inst. Metals **69**, 275 (1943).
[14]T. Gödecke and W. Köster, Z. Metallkd. **62**, 727 (1971).
[15]P. Guyot and M. Andier, Philos. Mag B **52**, L15 (1985).
[16]K. Kimura, T. Hashimato, K. Suzuki, K. Nagoyama, H. Ino, and S. Takenuchi, J. Phys. Soc. Jpn. **54**, 3217 (1985).
[17]J. Adams and J. B. Rich, Acta Crystallogr. **7**, 813 (1954).
[18]W. H. Jones, Jr., P. Graham, and R. G. Barnes, Phys. Rev. **132**, 1898 (1963).
[19]P. C. Taylor and P. J. Bray, Line shape Program Manual, 1969 (unpublished).
[20]W. G. Clark, Rev. Sci. Instrum. **35**, 316 (1964).
[21]G. C. Carter, L. H. Bennett, and D. J. Kahan, Prog. Mater. Sci. **20**, 1, (1977).